Stem Cell Reports, Volume *10*

Supplemental Information

Arginine Methylation Regulates MEIS2 Nuclear Localization to Promote Neuronal Differentiation of Adult SVZ Progenitors

Jasmine Kolb, Marie Anders-Maurer, Tanja Müller, Ann-Christin Hau, Britta Moyo Grebbin, Wiebke Kallenborn-Gerhardt, Christian Behrends, and Dorothea Schulte

Supplemental Figures

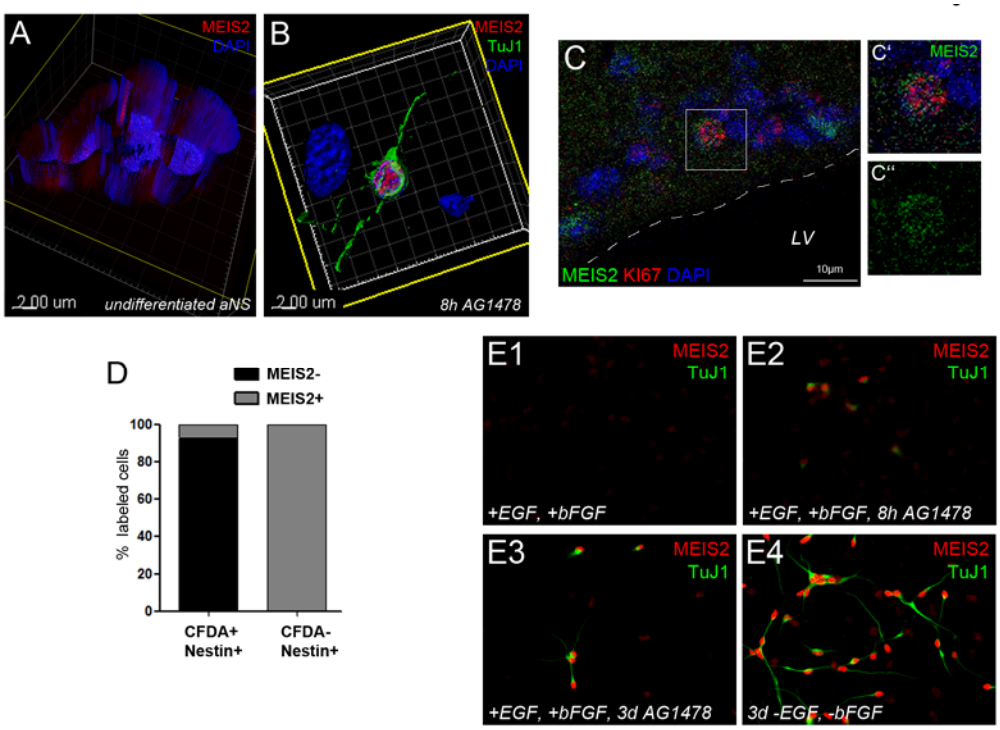

Figure S1. MEIS2 in adult SVZ-derived stem- and progenitor cells *in vivo* and *in vitro*. (A, B) 3D-reconstruction of serial confocal laser scanning micrographs of primary SVZ-derived aNS (A) or an *in vitro* differentiated TuJ1-labeled neuron obtained by plating on laminin and treatment with AG1478 (B). MEIS2-staining (red) is weak and not confined to the cell nucleus in adult neural progenitor cells, the primary component of aNS (A), but strong and nuclear in neurons, recognized by their immuno-reactivity for the TuJ1-epitope (green; B). (C) Weak, uniform MEIS2-staining in cells that exhibit nuclear Ki67-immunreactivity, presumably TAPs, in the SVZ *in vivo*. (D) Proportion of label-retaining (CFDA+) or label non-retaining (CFDA-), nestin-expressing cells that exhibit immunoreactivity for MEIS2. Putative transient amplifying cells (defined as CFDA-negative, nestin-expressing cells) exhibited uniform MEIS2-immunoreactivity in the cytoplasm and nucleus, whereas the vast majority of label-retaining, nestin-expressing cells (putative stem cells) did not stain for MEIS2. The few nestin+/CFDA+ cells that co-labeled with the MEIS2-specific antibody may either represent a minor population of label-retaining *Meis2*-expressing cells or, more likely, correspond to transient

amplifying cells that had been generated from label-retaining cells shortly before the cells were fixed and analyzed and therefore had not yet fully lost the CFDA-label. (E) Primary aNS grown as adherent cultures under different culture conditions; the images shown in panels 1-4 were taken with identical exposure times to highlight the strong increase in MEIS2 staining observed upon neuronal differentiation. (E1) MEIS2 immunoreactivity is very low in cells growing in the presence of EGF and FGF2; (E2) Addition of AG1478 elicits nuclear accumulation of MEIS2 in some cells of the culture, these cells stain positive for TuJ1; (E3) Appearance of TuJ1+ neurites in cells with nuclear MEIS2 staining upon prolonged differentiation times; (E4) typical staining for MEIS2 and TuJ1 in primary SVZ neurospheres differentiated for 3 days by withdrawal of EGF and FGF2 from the medium.

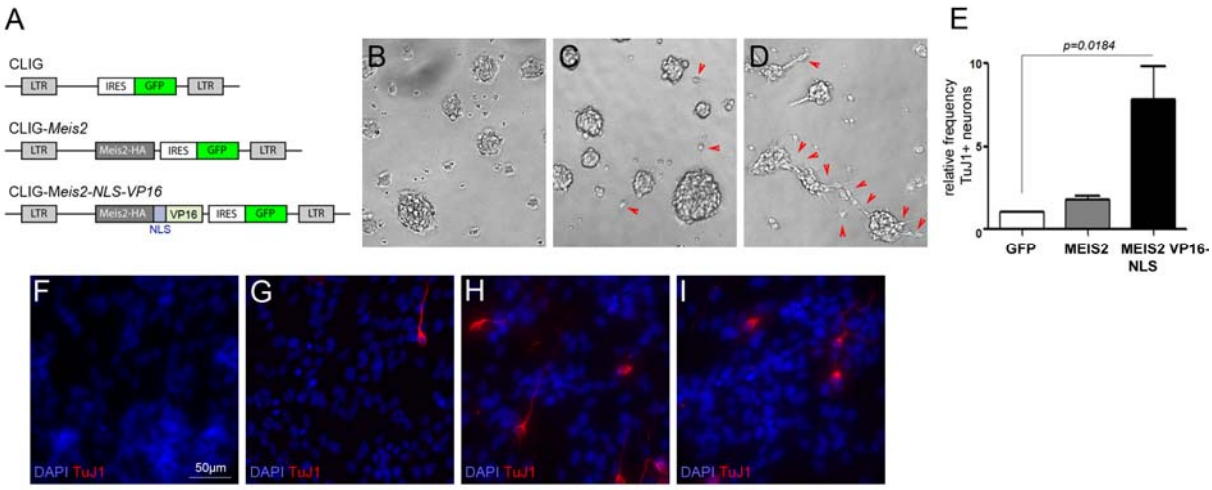

Figure S2. Retroviral misexpression of a transactivating fusion protein of *Meis2* in SVZ-derived aNS induces neuronal differentiation in EGF/FGF2 containing medium. (A) Schematic drawing of the retroviral vectors used. (B-D) Light microscopy images of aNS cultures growing as free-floating spheres in the presence of EGF and FGF2 and transduced with different viral vectors; viruses expressing only GFP (B), viral vectors carrying *Meis2* together with GFP (C), and viral vectors carrying *Meis2* C-terminally fused to a NLS and the VP16 transactivation domain (D). Red arrowheads indicate cells or groups of cells, which have attached to the cell culture flask and show the typical, bipolar morphology of differentiating neuroblasts. (E) Relative frequency of TuJ1+ neurons among cells transduced with the indicated retroviruses in aNS cultures growing in EGF/FGF2 containing medium. Transduction of *Meis2-VP16-NLS* induces substantial neuronal differentiation; n=3. Data are represented as mean ± SEM. (F-I) Representative, high-magnification images of TuJ1-immunoreactive cells generated from free-floating aNS growing in EGF/FGF2-containing medium and transduced with GFP (F), *Meis2* (G) or *Meis2-VP16-NLS* (H, I). The scale bar in (F) also applies to (G-I).

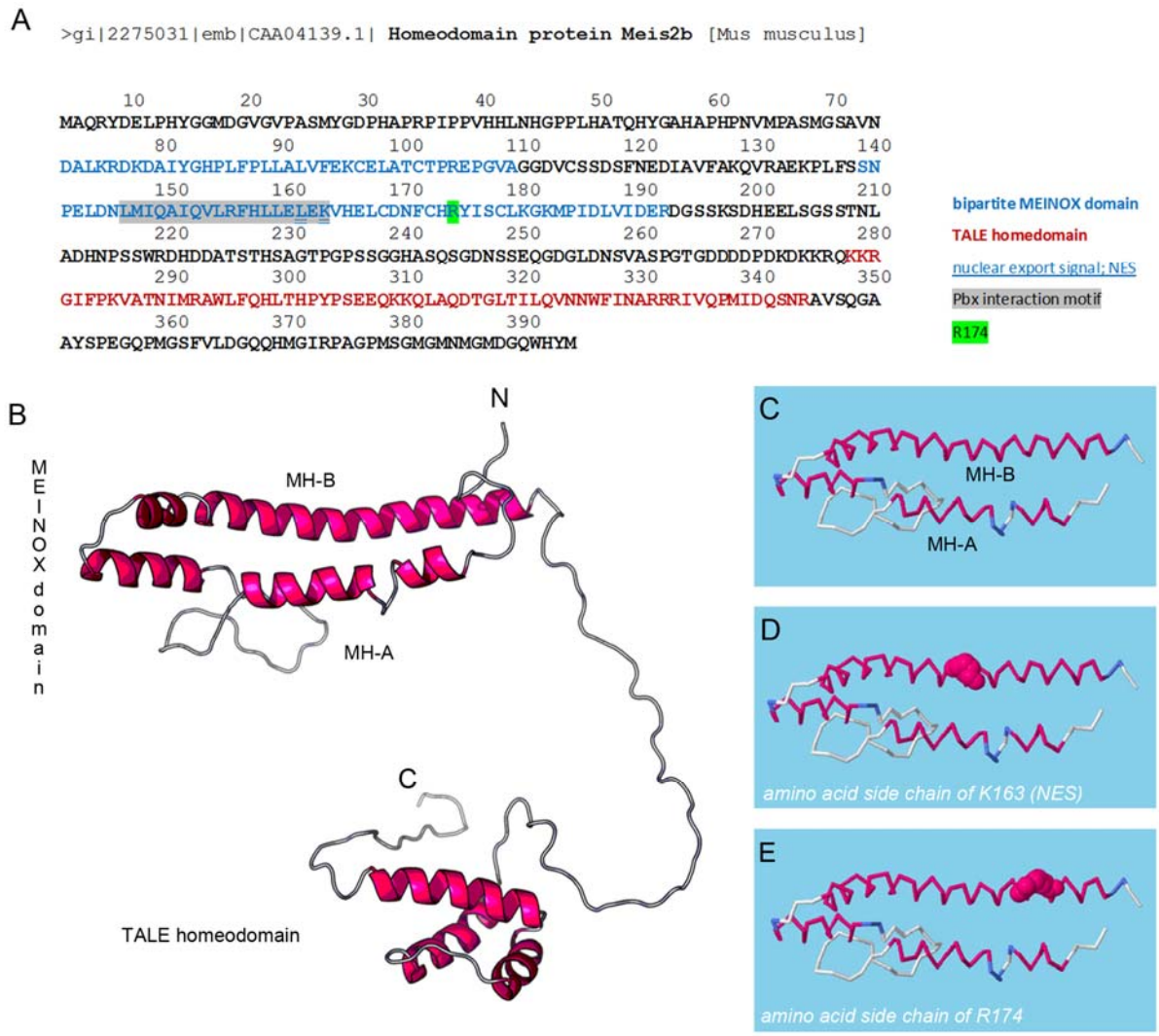

Fig. S3. Protein structure prediction of MEIS2. (A) Protein sequence of mouse MEIS2b; the bipartite MEINOX domain with the MH-A and MH-B subdomains is shown in blue, the TALE homeodomain in red. NES, the PBX-binding motif (as determined by (Knöpfler et al., 1997)) and R174 are underlined or shaded respectively. (B) Protein structure of MEIS2B as predicted by RaptorX (http://raptorx.uchicago.edu). (C-E) Schematic drawings of the MEINOX domain; the predicted orientation of the amino acid side chains of arginine 174 and lysine 163, an integral part of the LLELEK nuclear export motif, are shown in (E) and (D) respectively. Note that both amino acids are located within a predicted alpha helical structure with both side chains facing the same orientation.

Knoepfler, P.S., Calvo, K.R., Chen, H., Antonarakis, S.E., and Kamps, M.P. (1997). Meis1 and pKnox1 bind DNA cooperatively with Pbx1 utilizing an interaction surface disrupted in oncoprotein E2a-Pbx1. Proc. Natl. Acad. Sci. U.S.A. *94*, 14553-8.

Supplemental Experimental Procedures

Cultivation of primary stem-/progenitor cell cultures of the SVZ under free-floating and adherent conditions

All procedures involving animals were approved by the local animal care committee and the government of Hessen, and are in accordance with German and EU regulations. Neurospheres (aNS) were prepared from 7-10 week old C57bl6 mice and cultured in DMEM/F-12 containing 3.5 mM glucose (GIBCO), B-27 supplement (GIBCO), 20 ng/ml fibroblast growth factor-2 (FGF2, human recombinant; Peprotech) and 20 ng/ml epidermal growth factor (EGF, human recombinant; Peprotech) as described (Agoston et al., 2014). Unless noted otherwise, primary aNS, grown as free-floating spheres for no more than five days in the presence of EGF/FGF2 without attachment to laminin were used. To assess MEIS2 subcellular localization, aNS cells were split with accutase, resuspended in EGF/FGF2-containing culture medium and briefly allowed to attach to coverslips that had been coated with poly-D lysine. To induce cellular differentiation, aNS cells were split with accutase and plated on coverslips coated with (1µg/cm^2 laminin (Roche) in medium lacking EGF and FGF2 and cultivated for the times indicated. The images in Fig. S1E show adherent neurosphere cultures. For these, cells were allowed to attach to cell culture dishes coated with (1µg/cm^2 laminin (Roche), in EGF/FGF2-containing medium. For retroviral infection, neurospheres split with accutase, washed once with EGF/FGF2 containing medium, resuspended in 1.2ml EGF/FGF2 containing medium and incubated for 4 hours at 37^{o}C in the presence of retroviral stocks at 1-3x10^5 CFU/ml. Cells were then pelleted for 2min at 4.200 rpm in an Eppendorf centrifuge at room temperature, washed again once, resuspended in 5ml EGF/FGF2-containing medium and allowed to grow under non-adherent conditions for additional 48 hours. The following pharmacological agents were used: AdOX (Sigma Aldrich, A7154) 10µM (from a 1mM stock in distilled water); AG1478 (N-(3-Chlorophenyl)-6,7-dimethoxy-4-quinazolinamine; LC-Laboratories, T-7310) 100nM (from a 10mM stock in DMSO); SU5402 (3-[3-(2-Carboxyethyl)-4-methylpyrrol-2-methylidenyl]-2-indolinone; Santa

Cruz, sc-204308) 20µM (from a 10mg/ml stock in DMSO); Leptomycin B (Sigma, L2913) 50nM (from a 10µM stock in Methanol). Control cells were treated with equal volumes of the respective solvent.

Retroviral constructs

Full length Meis2b was amplified with the primers 5'-TACCAATTGCATGGCGCAAAGGTACGAT and 5'-TAGCTAGCCATATAGTGCCACTGCCCATC from cDNA prepared from the SVZ of adult C57Bl/6 mice and cloned MfeI and NheI into the EcoR1 and NheI sites of pSLAX13-HA (generous gift of Cliff Tabin, Harvard Medical School, Addgene #14027), which generates a C-terminal fusion to a triple HA-epitope to allow immunohistochemical differentiation between endogenous MEIS2 and the retrovirally misexpressed transgene. The mMeis2b-HA insert was isolated by XbaI digest, blunted and cloned into the pCLIG retroviral vector (Hojo et al., 2000). pCLIG carries an IRES-GFP cassette for visualization of the transduced cells. For CLIG-Meis2-NLS, an oligonucleotide corresponding to the nuclear localization signal of SV40 large T-antigen (PKKKRKV) (Kalderon et al., 1984) was inserted in frame into NdeI/SacI sites of the last HA-tag of mMeis2b-HA. For CLIG-MEIS2-NES, an oligonucleotide corresponding to the sequence LPPLERLTL (Fischer et al., 1995) was inserted in frame into NdeI/SacI sites of the last HA-tag of mMeis2b-HA. In CLIG-Meis2-NLS-VP16, mMEIS2b-HA was C-terminally fused to the NLS of SV40 large T-antigen followed by an in frame fusion to the herpes simplex virion protein 16 (VP16) transactivation domain. To generate CLIG-MEIS2-R174A the arginine at position 174 of mMeis2b-HA was converted into alanine by site directed mutagenesis (Phusion Site-Directed Mutagenesis Kit, Thermo Scientific, F-541) following manufacturer's instructions.

CFDA-labeling

Primary neurospheres were dissociated with accutase (Sigma Aldrich) 24 hours prior to labeling. CFDA labeling occurred in 2.5µM CFDA (carboxyfluorescein diacetat succinimidyl ester; Invitrogen, C1354) in Dulbecco's PBS (Invitrogen) for 5 min. at room temperature. Cells were washed in culture medium and once more after 1 hour of incubation at 37^{o}C. The cells were grown as free-floating aNS and passaged every three days by dissociation with accutase for a total of three passages. After the

last split, the cells were allowed to adhere to laminin coated slides, fixed in 2% paraformaldehyde in Dulbecco's PBS and stained with MEIS2- and nestin-specific antibodies.

Quantitative real-time PCR

Total RNA was isolated from murine SVZ-derived progenitor cells passage 1-2 utilizing RNeasy Mini Kit (Qiagen) including on-column DNase digestion (Qiagen, RNase-free DNase set) to eliminate remaining genomic DNA. RNA quality and quantity was assessed using a NanoDrop spectrophotometer. 1µg RNA was reversely transcribed with the First Strand cDNA Synthesis Kit (Thermo Scientific) with random hexamer primers according to the manufacturer's instructions. Complementary DNA corresponding to 5ng of total RNA was subjected to qPCR using ABsolute qPCR SYBR Green Mix (Thermo Scientific) and a CFX Real-Time PCR Detection System (BioRad). Relative target gene expression was normalized to the housekeeping gene β-actin. Relative expression was calculated with the ΔΔCq calculation method, normalizing first on housekeeping gene $\Delta Cq = Cq_{(TAR)} - Cq_{(REF)}$ followed by transformation to exponential expression $\Delta Cq = 2^{-\Delta Cq}$. Primer sequences were:

Meis1: 5`-TTGGAATTAGAGAAGGTACACGAA and 5`-TGGATAATTTGATGATACAAGCA;

Meis2: 5`-AGGTGATGACGACGATCCAG and 5´-GGCATTGATAAACCAGTTGTTCAC;

DCX: 5'- GGAAGGGGAAAGCTATGTCTG and 5'- TTGCTAGCCAAGGACTG;

β-actin: 5'- AGCCATGTACGTAGCCATCC and 5'-CTCTCAGCTGTGGTGGTGAA.

Antibodies and immunohistochemistry

The following primary antibodies were used: α-TUBULIN, mouse monoclonal (Abcam, ab-7291), WB (Western Blot): 1:40.000, IFC (immunofluorescence): 1:2.000; HA-HRP, rat monoclonal (3F10. Roche Diagnostics, 12 013 819 001), WB: 1:10.000; anti HA; rat monoclonal (3F10. Roche Diagnostics, 12 013 819 001) IFC 1:1.000; Ki67, mouse monoclonal (clone16A8, BioLegend, 652401**)** IFC: 1:200; MEIS2, rabbit polyclonal (gift of Arthur Buchberg, Arthur Buchberg, Kimmel Cancer Center, Pennsylvania), WB: 1:20.000, IFC: 1:5.000; MEIS2, mouse monoclonal (Sigma Aldrich, WH0004212M1), WB: 1:2.000, IFC: 1:200; NESTIN mouse monoclonal b (Chemicon, MAB252), IFC

1:500; neuronal βIII-TUBULIN (TuJ1), mouse monoclonal (Covance, MMS-435P), IFC: 1:1.000; PBX1, rabbit polyclonal (Cell Signaling Technologies, 4342) WB: 1:1.000, IFC: 1:400; PREP1 / MEIS4 clone 1.1, mouse monoclonal (Upstate, 05-766) WB: 1:10.000; PSA-NCAM, mouse monoclonal (Millipore, MAB5324), IFC 1:1.000. Secondary antibodies for immunohistochemistry were Alexa 594-, Alexa 488-, Cy2 or Cy3 conjugated (Molecular Probes, OR, Invitrogen, Karlsruhe, Germany or Dianova, Hamburg, Germany). Some sections were counterstained with 4'-6-Diamidino-2-phenylindole (DAPI) to visualize cell nuclei. For immunostaining, cells or fresh cryosections were fixed for 10 min. at room temperature in 2% paraformaldehyde in Dulbecco's PBS, washed in PBS and stained over night in the presence of 5 % ChemiBlock (Millipore) or 10 % goat serum with 0.5 % Triton X 100 and the antibodies listed above. SDS-PAGE and Western Blot were performed following standard protocols.

Analyses of MEIS2-containing protein complexes

Subcellular fractionation, immunoprecipitation and GST pull-down assays were performed as described (Agoston and Schulte, 2009; Agoston et al., 2014). For immunoprecipitation (except purification of MEIS2 for mass spectrometry, see below), 2µg per reaction of the following antibodies were used: HA-probe, rabbit polyclonal (Santa Cruz Biotechnology, Y-11), PBX1, rabbit polyclonal (Cell Signaling Technologies, 4342), MEIS2, goat polylconal (Santa Cruz Biotechnoloy, sc-10600). Isotype specific antibodies served as control (Santa Cruz Biotechnology). Secondary antibodies were Alexa 350-, Alexa 488-, Alexa 568-, Alexa 594- or Cy5-conjugated (Molecular Probes). For Western Blot analysis, proteins were separated on SDS-PAGE, transferred onto PVDF-membranes, blocked and incubated with the above antibodies following standard methods. HRP-conjungated secondary antibodies were goat-anti rabbit HRP (Cell Signaling Technologies, 1:10.000), goat-anti mouse HRP (Sigma Aldrich, 1:10.000), Immunocruz anti-mouse (Santa Cruz Biotechnology). Antibodies were diluted in 3% BSA in Tris-buffered saline or Rotiblock (Carl Roth, Karlsruhe, Germany). Blots were developed with Luminata forte (Millipore), chemiluminescence signals were detected with a LI-COR Odyssey Fc imager.

Mass-spectrometry analysis

MEIS2 protein from aNS and OB tissue was isolated by immunoprecipitation from the olfactory bulbs of eight 10-week old C57Bl/6 mice or early secondary aNS produced from 10 age matched C57Bl/6 mice per experiment. For MEIS2 isolation from aNS, primary aNS were dissociated with accutase (Sigma Aldrich) one day prior to extract preparation and $4x10^7$ cells per experiment were allowed to recover over night. Preparation of cytoplasmic and nucelar extract and immunoprecipiation of MEIS2 were carried out as described (Agoston et al., 2014) and with 31.2µg anti-MEIS1/2 goat (Santa Cruz Biotechnology; sc-10599-X) and 120µg protein A dynabeads (Invitrogen) per reaction. Preparation of protein extracts from aNS was carried out in the presence of 5µM MG123 (Merck, 474791). Precipitates were separated by SDS-PAGE, stained with Colloidal Coomassie and the MEIS2 protein band was excised from the gel.

Liquid chromatography-tandem mass spectrometry analyses were performed on an EasyLC nano-HPLC coupled to an Orbitrap Elite mass spectrometer (both Thermo Scientific). In gel trypsin digestion of the immunoprecipitates was performed as described previously (Shevchenko et al., 2006). Briefly, eluates were run on a SDS-PAGE, alkylated with chloroacetamide, overnight digested with trypsin (Promega), and extracted. The desalted peptide mixtures were injected onto the column in HPLC Solvent A (0.5% acetic acid) and eluted with a 5%‑33% gradient HPLC solvent B (80% acetonitril in 0.5% acetic acid) running at a constant flow rate of 200 nl/min at 30°C. Full-scan MS spectra were acquired in a mass range from m/z 150 to 2,000 with a resolution of 120.000 without lock mass. The 20 most intense precursor ions were sequentially CID fragmented in each scan cycle. In all measurements, up to 500-sequenced precursor masses were excluded from further analysis for 90 s. The target values of the mass analyzers were 1 million charges (MS) and 5,000 charges (MS/MS). MS data was processed using default parameters of the MaxQuant software (1.2.2.5) (Cox and Mann, 2008). The peak lists were queried against the human UniProt database (2012_04). Full tryptic specificity was required, and up to two missed cleavages were allowed. Carbamidomethylation of cysteine was set as fixed modification. Protein N-terminal acetylation,

oxidation of methionine, and methylation of arginine and lysine were set as variable modifications. Initial precursor mass tolerance was set to 7 ppm and 0.5 Da at the fragment ion level. False discovery rates were set to 1% at peptide and protein group level. The MS/MS spectra shown in Fig. 4 represent MEIS2 isolated from cytoplasmic extracts prepared from aNS (Fig. 4A) and nuclear extracts of OB tissue (Fig. 4B). R174 was neither methylated in MEIS2 precipitated from nuclear nor cytoplasmic aNS extracts. No MEIS2 protein could be detected in cytoplasmic OB-extracts.

Peptide pull-down

Peptides comprising the sequences LM**I**QAIQV**L**RFH**L**LE**L**EKVHELCDNFCHRYISCLK and LM**I**QAIQV**L**RFH**L**LE**L**EKVHELCDNFCHR{met}YISCLK, N-teminally linked to a mini-PEG linker followed by biotin were purchased from ProteoGenix (Schiltigheim, France). Peptides were immobilized on streptavidin-coated dynabeads (Invitrogen) essentially as described in (Dormann et al., 2012) with the following modifications: 200 pmol peptide per 10 µl beads were coupled in binding buffer (20mM sodium phosphate buffer pH 7.4, 150mM KCl, 0.5mM EDTA, 5mM MgCl2, 10% Glycerol, complete protease inhibitor cocktail (Roche)). Beads were washed four times in blocking buffer (binding buffer supplemented with 0.1% BSA), blocked for 12 min and washed once in binding buffer supplemented with 0.01% Tween20. Recombinant PBX1 and CRM1-HA were generated from pCS2-Pbx1a (gift of L. Selleri, Weill Cornell Medical College) and pRK5-Crm1HA (gift of R. Kehlenbach University Medical School Göttingen (Roloff et al., 2013)) respectively by TNT-coupled transcription/translation following the manufacturer's instructions (Promega). 60µl reactions each were diluted to 600 µl with water and increasing volumes of the respective proteins were incubated with 10µl peptide-coupled beads for 2 hours at 4^{o}C. Thereby, 1 arbitrary unit (a.u.) in Figs. 3 and 4 corresponds to 10µl of the diluted *in vitro* translated proteins (e.g. 6 a.u. equal 60µl (or 10%) of the 600µl IVT reaction). For competitive pull-down assays, 30µl PBX1 were incubated with the beads for 30 min prior to addition of the indicated amounts of CRM1-HA. After the incubation period, the beads were washed four times with binding buffer supplemented with 0.01% Tween20; bound proteins were eluted in 1x LDS-

sample buffer (Novex) and heated to 95°C for 5 min. This treatment also removed the biotinylated peptides from the streptavidin matrix. Eluted proteins and peptides were separated on a 8-16% Tris-Glycine gradient gel (Novex), transferred to PVDF-membranes and detected with antibodies specific for PBX1 and the HA-epitope respectively. Blots were stripped and re-probed with streptavidin-HRP to detect the biotinylated peptides. For the graph shown in Fig. 4O, band intensities were quantified with ImageJ and normalized to the band achieved with 10µl of the diluted *in vitro* translated proteins (i.e. input of 1 a.u.).

Reporter assay

The luciferase reporter construct DCX2073 contains the genomic fragment of NT -3838 to NT -1765 upstream of the DCX start codon (corresponding to pdcx2kb of (Piens et al., 2010)) subcloned into pGL3basic (Promega) and was previously described in Agoston et al., 2014. HEK293T cells were chosen for reporter assays because of their low endogenous Meis2 expression. Cells were transfected with 140ng of the above reporter constructs together with 40fmol each of Pbx1b-pCS2+, Meis2b-pMIWIII and Pax6(-5a)-pMIWIII. A plasmid expressing Renilla luciferase under the control of the human elongation factor 1 (Hef-1) promoter was co-transfected for normalization, luciferase assays were performed in triplicates 48 hours after transfection according to (Dyer et al., 2000).

In silico analysis of protein motifs

The NES motif in MEIS2 was identified according to (Cour et al., 2004) (http://www.cbs.dtu.dk/services/NetNES/). NLS sequences were analyzed based on models by Kosugi and colleagues (http://nls-mapper.iab.keio.ac.jp/cgi-bin/NLS_Mapper_form.cgi; (Kosugi et al., 2008; 2009a; 2009b)). Protein seconday structure prediction was carried out using Psipred (http://bioinf.cs.ucl.ac.uk/psipred/) and RaptorX (http://raptorx.uchicago.edu/; (Källberg et al., 2012).

Data acquisition and statistical analysis

Images were taken with a Nikon 80i, confocal images with a Nikon Eclipse TE2000-E and a 63 oil immersion lens with optical sections of maximum 1–2 µm intervals. A minimum of 300 cells per condition and experimental repeat were photographed. The number of independent experiments is given in the figure legends as 'n= *number of independent experiments*'. Standard deviation was calculated between independent experiments. Error bars represent s.e.m. Comparison between two groups was performed with unpaired student's t-test or non-parametrical Mann-Whitney U test when normal distribution of the data could not be assumed. Comparison between three or more groups was carried out by one-way ANOVA followed by Bonferoni Multiple Comparison post-hoc test (Prism 5.01, Graph Pad). Because the immunohistochemical staining intensity for MEIS2 obtained in primary aNS is significantly lower than that seen in *in vitro* differentiated neurons, neurons of the OB or in SK-N-Be(2) cells, contrast settings had to be adjusted automatically across the entire image to visualize the subcellular distribution of MEIS2 protein in aNS. The intensities of the MEIS-specific immunofluorescence shown in Fig.1B-G, 2B, C, and 4C, D, F, G, J, K therefore slightly overestimate the actual MEIS2 protein present in the cells. An unbiased account of the relative protein expression levels of MEIS2 in undifferentiated, SVZ-derived progenitor cells and differentiated neurons can be seen in Fig. $S1E_1$-E_4, which show aNS grown as adherent cultures on laminin (Fig. $S1E_1$) and at different times after cellular differentiation was induced by addition of AG1478 (Fig. $S1E_2$, $S1E_3$) or removal of EGF and FGF2 from the culture medium (Fig. $S1E_4$).

Supplemental references

Agoston, Z., and Schulte, D. (2009). Meis2 competes with the Groucho co-repressor Tle4 for binding to Otx2 and specifies tectal fate without induction of a secondary midbrain-hindbrain boundary organizer. Development *136*, 3311-22.

Agoston, Z., Heine, P., Brill, M.S., Grebbin, B.M., Hau, A., Kallenborn-Gerhardt, W., Schramm, J., Götz, M., and Schulte, D. (2014). Meis2 is a Pax6 co-factor in neurogenesis and dopaminergic periglomerular fate specification in the adult olfactory bulb. Development *141*, 28-38.

Cour, T.L., Kiemer, L., Mølgaard, A., Gupta, R., Skriver, K., and Brunak, S. (2004). Analysis and prediction of leucine-rich nuclear export signals. Protein Engineering, Design &Amp; Selection : PEDS *17*, 527-36.

Cox, J., and Mann, M. (2008). MaxQuant enables high peptide identification rates, individualized p.p.b.-range mass accuracies and proteome-wide protein quantification. Nature Biotechnology *26*, 1367-72.

Dormann, D., Madl, T., Valori, C.F., Bentmann, E., Tahirovic, S., Abou-Ajram, C., Kremmer, E., Ansorge, O., Mackenzie, I.R.A., Neumann, M., et al. (2012). Arginine methylation next to the PY-NLS modulates Transportin binding and nuclear import of FUS. The EMBO Journal *31*, 4258-75.

Dyer, B.W., Ferrer, F.A., Klinedinst, D.K., and Rodriguez, R. (2000). A noncommercial dual luciferase enzyme assay system for reporter gene analysis. Analytical Biochemistry *282*, 158-61.

Fischer, U., Huber, J., Boelens, W.C., Mattaj, I.W., and Lührmann, R. (1995). The HIV-1 Rev activation domain is a nuclear export signal that accesses an export pathway used by specific cellular RNAs. Cell *82*, 475-83.

Hojo, M., Ohtsuka, T., Hashimoto, N., Gradwohl, G., Guillemot, F., and Kageyama, R. (2000). Glial cell fate specification modulated by the bHLH gene Hes5 in mouse retina. Development *127*, 2515-22.

Kalderon, D., Roberts, B.L., Richardson, W.D., and Smith, A.E. (1984). A short amino acid sequence able to specify nuclear location. Cell *39*, 499-509.

Kosugi, S., Hasebe, M., Entani, T., Takayama, S., Tomita, M., and Yanagawa, H. (2008). Design of peptide inhibitors for the importin alpha/beta nuclear import pathway by activity-based profiling. Chem. Biology *15*, 940-9.

Kosugi, S., Hasebe, M., Matsumura, N., Takashima, H., Miyamoto-Sato, E., Tomita, M., and Yanagawa, H. (2009a). Six classes of nuclear localization signals specific to different binding grooves of importin alpha. J. Biol. Chem. *284*, 478-85.

Kosugi, S., Hasebe, M., Tomita, M., and Yanagawa, H. (2009b). Systematic identification of cell cycle-dependent yeast nucleocytoplasmic shuttling proteins by prediction of composite motifs. Proc. Natl. Acad. Sci. U.S.A. *106*, 10171-6.

Källberg, M., Wang, H., Wang, S., Peng, J., Wang, Z., Lu, H., and Xu, J. (2012). Template-based protein structure modeling using the RaptorX web server. Nature Protocols *7*, 1511-22.

Piens, M., Muller, M., Bodson, M., Baudouin, G., and Plumier, J. (2010). A short upstream promoter region mediates transcriptional regulation of the mouse doublecortin gene in differentiating neurons. BMC Neuroscience *11*, 64.

Roloff, S., Spillner, C., and Kehlenbach, R.H. (2013). Several phenylalanine-glycine motives in the nucleoporin Nup214 are essential for binding of the nuclear export receptor CRM1. J. Biol. Chem. *288*, 3952-63.

Shevchenko, A., Tomas, H., Havlis, J., Olsen, J.V., and Mann, M. (2006). In-gel digestion for mass spectrometric characterization of proteins and proteomes. Nature Protocols *1*, 2856-60.